Metastable states in the triangular-lattice Ising model studied by Monte Carlo simulations: Application to the spin-chain compound $Ca_3Co_2O_6$

R. Soto,[1] G. Martínez,[1,2,*] M. N. Baibich,[2] J. M. Florez,[1,3] and P. Vargas[1,4,†]
[1]*Departamento de Física, Universidad Técnica Federico Santa María, Casilla 110-V, Valparaíso, Chile*
[2]*Instituto de Física, Universidade Federal do Rio Grande do Sul, 91501-970 Porto Alegre, RS, Brazil*
[3]*Materials Science and Engineering, Massachusetts Institute of Technology, Cambridge, Massachusetts 02139, USA*
[4]*Max-Planck-Institut für Festkörperforschung, Heisenbergstrasse 1, D-70569 Stuttgart, Germany*
(Received 18 September 2008; revised manuscript received 9 February 2009; published 20 May 2009)

It is well known that the spin-chain compound $Ca_3Co_2O_6$ exhibits interesting plateaus in the magnetization as a function of the magnetic field at low temperatures. The origin of them is still controversial. In this paper, we study the thermal behavior of this compound with a single-flip Monte Carlo simulation on a triangular lattice and demonstrate the decisive influence of metastable states on the splitting of the ferrimagnetic 1/3 plateau below 10 K. We consider the $[Co_2O_6]_n$ chains as giant magnetic moments described by large Ising spins on planar clusters with open boundary conditions. With this simple frozen-moments model we obtain stepped magnetization curves which agree quite well with the experimental results for different sweeping rates. We describe particularly the out-of-equilibrium states that split the low-temperature 1/3 plateau into three steps. They relax thermally to the 1/3 plateau, which has long-range order at equilibrium. Such metastable states are further analyzed with snapshots unveiling an interlinked mobile domain walls structure that is responsible for the observed behavior of the 1/3 plateau. A comparison is also given of our classical Monte Carlo results with exact diagonalization results in small triangular quantum clusters, providing further support for our thermal description of this compound.

DOI: 10.1103/PhysRevB.79.184422 PACS number(s): 75.25.+z, 75.30.Kz, 75.40.Mg, 75.60.−d

I. INTRODUCTION

Low-dimensional interacting spin systems always reveal very interesting magnetic properties, as well as new electronic transport phenomena.[1–4] Along this line, systems with geometric frustration have long attracted our attention because ground-state properties, like their degeneracy, are usually responsible for peculiar behaviors at low temperatures. Included are exotic magnetization dependences with external fields in hysteresis curves, for example. One group of compounds that exhibits such properties is the family $CsCoX_3$, where X stands for Cl or Br.[5] These materials are quasi-one-dimensional Ising-type magnetic systems. The spin chains are arranged on a triangular lattice, while the intrachain and interchain exchange couplings are both antiferromagnetic.

Another fascinating spin-chain family of compounds with triangular arrangements has the formula A'_3ABO_6 (where A' may be Ca or Sr, whereas A and B are transition metals). One particular system that caught our attention is $Ca_3Co_2O_6$,[6–24] which has a rombohedral structure composed of large chains of $[Co_2O_6]_n$ along the c axis of a corresponding hexagonal lattice. The Ca atoms are located among those chains. The chains are made of alternating face-sharing CoO_6 trigonal prisms and CoO_6 octahedra. Each Co chain is thus surrounded by six equally spaced Co chains forming a hexagonal lattice in the ab plane (see Fig. 1).

In $Ca_3Co_2O_6$ the long Co-Co interchain distance (5.3 Å), as compared to the short Co-Co intrachain distance (2.6 Å), ensures the hierarchy of the magnetic exchange energies, $J_{\text{intra}} \gg J_{\text{inter}}$, in modulus. This fact, together with a strong spin-orbit coupling,[25,26] provide a high uniaxial anisotropy along the c axis. Neutron diffraction studies,[7] among others, have revealed a ferromagnetic intrachain interaction ($J_{\text{intra}} < 0$), while an antiferromagnetic interchain interaction ($J_{\text{inter}} > 0$) was observed in the ab plane. Consequently, it is very plausible to describe the magnetism of this compound by considering an Ising triangular lattice of large rigid moments linked to the chains, each one playing the role of a giant spin, pointing either up or down.

One of the interesting features observed in $Ca_3Co_2O_6$ is the appearance of plateaus in the magnetization curve M vs H, below $T_C = 25$ K, when the magnetic field is applied along the chains (c axis). For temperatures in the range, $10\ \text{K} \leq T \leq T_C$, a rapid increase in M with H is observed. Close to zero field, the magnetization reaches a plateau at the value of $M_s/3$ (M_s, the saturation magnetization is $\sim 4.8 \mu_B$/f.u.). This value remains constant up to $H_c \approx 3.6$ T, where the magnetization springs up to its saturation value M_s. On the other hand, when $T \leq 10$ K, namely

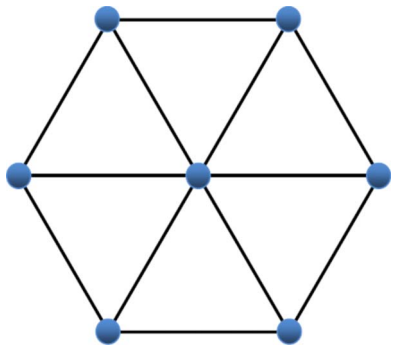

FIG. 1. (Color online) Hexagonal lattice of Co chains (blue or filled dots) projected onto the ab plane of the spin-chain compound $Ca_3Co_2O_6$. Each chain is ordered ferromagnetically and is weakly coupled antiferromagnetically to its neighbors.

the ferrimagnetic region, the observed plateau at $M_s/3$ splits up into three small steps, changing at fields $H=1.2$, 2.4, and 3.6 T, respectively. Much effort has been made to understand such behavior and it is still a controversial matter. Some papers[16,21,24] raised the question that this behavior might be related to other experiments involving single-molecule magnets (SMM),[27,28] where the quantum effect, called quantum tunneling of the magnetization (QTM), is realized.[29] We restrict such a statement to temperatures above 4 K, as we demonstrate in this work, and leave open the question of QTM effects to be searched below 2 K.

We follow instead the line of reasoning that metastable states, or peculiar mozaic configurations, might play a role in the splitting of the magnetization of this frustrated material, as first suggested by Maignan *et al.*[9] Therefore, we started a simulation along the lines given by Kudasov,[30] who predicted an opening of the 1/3 plateau using Monte Carlo analysis at $T=0$. More recently, Yao *et al.*[31,32] studied this compound with numerical Monte Carlo simulations on finite clusters. The latter works describe the system with an Ising Hamiltonian on a triangular lattice, using periodic boundary conditions. Despite the fact their results reproduce the right steps width ($\Delta H \sim 1.2$ T), in the magnetization curves, they do not find a clear-cut (*equilibrium*) configuration that explains the splitting of the 1/3 plateau. In this work, we report on a similar study using the same model, but considering instead free boundary conditions on an anisotropic system, which is added for completion with the intrinsic dipolar term at the end. We apply nonequilibrium techniques to this system. We detect in this form, by sweeping the field at different rates, the presence of metastable domain walls that perfectly explain the observed trends of the splitting of the 1/3 plateau at low temperatures and verify that the latter has long-range order at equilibrium.

To be consistent with the previous existing models, we use the same set of parameters for the Hamiltonian,[30–32] namely, an interchain antiferromagnetic interaction, $J=J_{\text{inter}}=2.25$ μeV, and a large Ising magnetic moment, $S=32$. The fact of having a giant magnetic moment of modulus $S=32$ is related to an estimate of the length of the Co chains in the experiments, although we have no data to compare with. Disorder or dispersive effects in the exchange coupling constant were also not required to obtain the splitting of the 1/3 plateau, as it will become clear in the following. Therefore, our model and methods are different from Yao *et al.*,[31,32] and we concentrate our efforts mainly to describe the effects of the field sweep rate on the observed metastable states that generate the plateaus in the magnetization.

II. MONTE CARLO SIMULATIONS IN TWO DIMENSIONS

The spin-chain compound $Ca_3Co_2O_6$ is formed by close-packed one-dimensional parallel chains arranged along the c axis. These chains span a triangular lattice over the ab plane, as it is shown in Fig. 1. Due to such geometric configuration and the hierarchy of the exchange interactions, the system can be modeled as a two-dimensional (2D) antiferromagnetic Ising model with nearest-neighbor exchange interactions.[30–32] The magnetic moments are representative of the $[Co_2O_6]_n$ chains, which are always perpendicular to the ab plane. The choice of this frozen-moments model is a consequence of a time-scale assumption. We believe that the characteristic time involved in reversing the individual spins of each chain is much shorter than the rearrangement of the triangular lattice by changing the magnetic field. This hypothesis is based on our previous numerical results on nanowires,[33,34] as well as on the large number of sites that are involved in changing the whole triangular lattice if compared to those on a single spin chain.

We thus performed Monte Carlo simulations using a triangular Ising model, where giant magnetic moments of moduli $S=32$ are frozen, pointing either up or down, and coupled antiferromagnetically ($J>0$) to their six nearest neighbors. In this picture, the Hamiltonian $\mathcal{H}$ of the system is

$$\mathcal{H} = \frac{1}{2} J \sum_{\langle i,j \rangle} S_i^z S_j^z - g \mu_B H \sum_i S_i^z, \tag{1}$$

where S_i^z is the spin of each magnetic moment, H is the external magnetic field along the $+c$ axis, $g=2$ is the electronic Landé factor, μ_B is the Bohr magneton, and $\langle i,j \rangle$ indicates summation over all pairs of nearest neighbors on a triangular lattice. We used a single-flip Monte Carlo method together with the standard Metropolis algorithm to reject or accept spin flips in the magnetization with a Boltzmann factor.[35] Magnetization measurement at any given field was done using 1000 averages over a fixed number of *accepted* Monte Carlo flips (MCF). We used different 2D finite cluster configurations, including superhexagons, octagons, dodecagons, and other more circularly shaped geometries to represent the samples. The magnetization curves found in all these finite clusters were very similar, the main difference was the number of MC flips needed to reach the plateaus for different sizes. For visualization aspects, a selection of the results for one particular cluster size with hexagonal geometry was chosen. Extra material showing the time evolution of magnetic configurations along the field can be found at the website by the interested reader (see supplementary material in Ref. 36).

III. MAGNETIZATION RESULTS

In this section we discuss our magnetization results by using Monte Carlo calculations on finite clusters with open boundary conditions, always increasing the field. The initial state at zero field was obtained by thermalizing a randomly disordered configuration, performing 10^6 MCF in a *training* period. Thereafter, we started to increase the field in steps of $\Delta H=0.075$ T at a constant sweep rate. We calculated large clusters with hexagonal geometries for $N=1387$, 2431, 3169, 4921, and 6931 sites, respectively. Some larger clusters were also calculated, but we verified that the results did not change appreciably with size; as the system increased the plateaus structure remained unaltered, with small perturbations (substeps) on some of the three main plateaus which tended to disappear for larger N.

In Fig. 2, done for a sweep rate of 10^4 MCF, we observe the formation of three well-defined plateaus below T

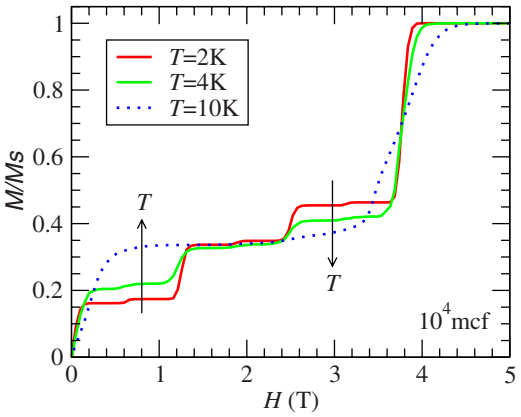

FIG. 2. (Color online) MC results for the magnetization as a function of the applied field for different temperatures, at a fixed rate of 10^4 MCF, in the ferrimagnetic phase ($T \leq 10$ K), for $N=2431$ sites. The split up of the 1/3 plateau into three successive plateaus is observed below 10 K. They extend up to fields $H \approx 1.2$, 2.4, and 3.6 T, respectively. We see that they merge into a unique plateau (dotted curve) at $M \approx M_s/3$ as T increases. They rise to saturation with different slopes.

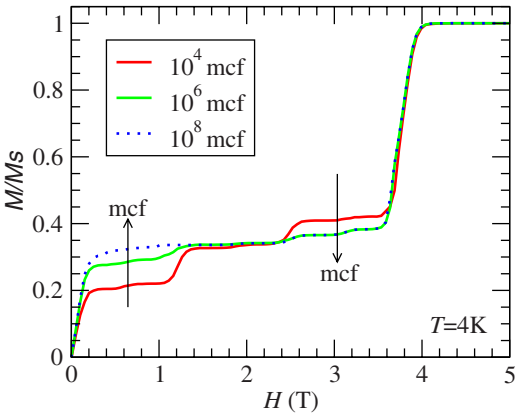

FIG. 3. (Color online) MC results for the magnetization as a function of the applied field for different sweep rates, at $T=4$ K, and for $N=2431$ sites. This is accomplished by letting more or less accepted MC flips (MCF) per magnetic field in the simulation. Notice the tendency of the plateaus to merge into the plateau $M_s/3$ (dotted curve) as the number MCF increases, indicating a time decay toward the 1/3 state. This behavior will be further analyzed in the text.

$=10$ K. Important to see is that they merge into one at $M_s/3$ as T increases, indicating close resemblance with the experimental situation (see, e.g., Fig. 3 in Ref. 19). The presence of extra tiny substeps is an unavoidable boundary effect due to the finiteness of the cluster used (in this case, $N=2431$ sites). They are created by border isolated atoms whose magnetic contribution is strongly suppressed for larger cluster sizes, and are therefore irrelevant for our argument. Another important feature seen in Fig. 2, and shared by experiments, is the steeper rise of the magnetization for lower temperatures at the end of the 1/3 plateau (see curve $T=2$ K close to $H_c \approx 3.6$ T).

Now, as a way to check how stable are such plateaus, we have performed various numerical analyses with an increasing number of Monte Carlo steps per magnetic field. In fact, as the simulation is done with the accepted configurations, what really counts is MCF and not Monte Carlo steps (mcs). We clearly see, in Fig. 3, the tendency of the three split plateaus to merge into one plateau at $M_s/3$ as the number of MCF increases. This feature must be related to the experimental sweep rate, as in Ref. 19. Such a connection allows us to say that the three split plateaus are metastable states and are, therefore, a dynamical effect; for this very reason the experimental magnetization curves are strongly dependent on the sweeping rate.

This merging effect can be better understood in the picture of Fig. 4, where we have obtained an almost perfect superposition between magnetization curves of different temperatures and, at the same time, of different MCF. In such a case, we tried to draw a parallel between the MCF in our simulation and the sweep rate in the experimental results,[19] where this behavior is also observed. It is obvious from this result the strong interplay between the effects of time and temperature (see, e.g., Fig. 4 in Ref. 19), a feature which was previously used as a fingerprint of QTM. Although MCF are *not* related to laboratory time measurement, we can assign them to some sweep rate by comparing the formation of the plateaus. Hence, we can say that the three split plateaus are made of metastable states, which evolve in time to the 1/3 plateau for lower sweep rates (i.e., higher MCF), as in Fig. 3.

Dipolar interactions were also considered, as an intrinsic effect always present in nanowires and other low-dimensional systems, but its overall effect here was merely to induce an effective antiferromagnetic field that retarded the field at which the steps occur. The dipolar term $\mathcal{H}_{\text{dip}}$ that was added to Eq. (1) is given by

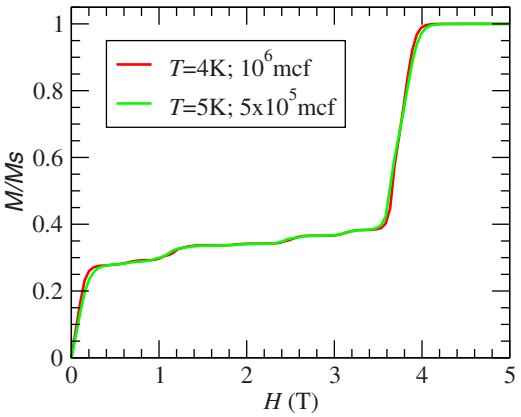

FIG. 4. (Color online) Magnetization versus applied field for two different temperatures with different sweep rates. Notice that both curves almost merge into one, indicating that they correspond to the same statistical configuration, one that gives similar magnetic moments. Such *scaling* is an extra indication of metastable configurations. Small differences are seen at the steep rising regions, close to zero and at $H_c \approx 3.6$ T, a fact which is also shared by the experiments (see Ref. 19).

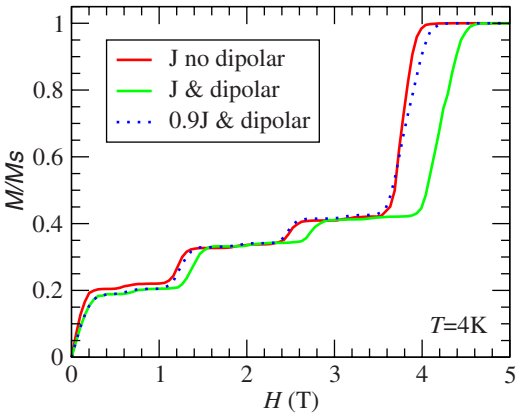

FIG. 5. (Color online) Magnetization versus applied field with dipolar interactions, at $T=4$ K, and for $N=2431$ sites. The red (dark) curve is the same as in Fig. 3 (10^4 MCF), without dipolar interaction. The green (light) curve includes now the dipolar interaction, while the blue (dotted) curve is with dipolar interaction but of a reduced exchange, 90% of the original J value. We see that the scaling of the red (dark) and the blue (dotted) curves is not perfect but is very close.

$$\mathcal{H}_{\text{dip}} = \frac{1}{2}\sum_{i,j} \frac{\mathbf{m}_i \cdot \mathbf{m}_j - 3(\mathbf{m}_i \cdot \hat{\mathbf{r}}_{ij})(\mathbf{m}_j \cdot \hat{\mathbf{r}}_{ij})}{r_{ij}^3}, \qquad (2)$$

where the summation is over all sites, and $\mathbf{m}_i = \pm \mu_B \mathbf{S}_i$. We see such effect in Fig. 5, with the dipolar interaction playing the role of an effective antiferromagnetic field, $H \rightarrow H + H_{\text{eff}}$ added to Eq. (1), that shifts the magnetization curves to the right. We have noticed that adjusting the exchange constant to $0.9J$, we can almost match these results with the previous calculations, without dipolar interaction (see Fig. 5). For this reason, we think, the magnetization curves are well described using only the exchange and Zeeman terms.

IV. SNAPSHOTS AND DOMAIN WALLS

The physics behind these results can be visualized by using raw snapshots of selected configurations. In the next pictures, we will show different snapshots of the magnetization patterns for the parameters of the red curve in Fig. 3, namely, 10^4 MCF and $T=4$ K. They were taken at three different magnetic fields: $H=0.81$ T, $H=2.0$ T, and $H=2.98$ T, representative of the center of each plateau of the ferrimagnetic phase, respectively.

Our color convention to analyze the snapshots of the subsequent examples is depicted in Fig. 6. Following Ref. 9, we defined four triangles and colored them differently depending on the magnetization that results by summing up the three spins at their vertices (cf. Fig. 6).

Thermalized configurations at zero field are formed mostly by disordered bicontinuous patterns of orange (light) and green (gray) phases, in a 1:1 proportion, with zero total magnetization. For magnetic fields close to 0.25 T, fast-moving domain walls, similar to those seen in Fig. 7 in orange (light) color, stabilize their motion becoming quasistatic interlinked domain walls, until the field is close to 1.2 T. The

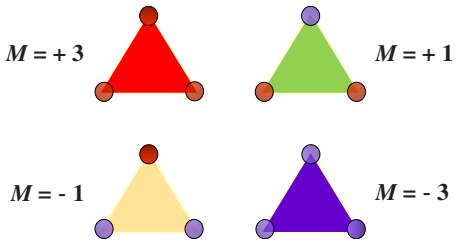

FIG. 6. (Color online) The magnetic moment of each triangle depends on the orientation of each ferromagnetic chain. The four possibilities are here schematized by different colors (gray scales), but the case $M=-3$ is seldom seen for positive magnetic fields in the following snapshots.

configuration shown in Fig. 7 contributes to a total magnetization $M=0.22M_s$.

Moving the field across the boundary, $H=1.2$ T, produces a rapid fluctuation of the domain walls, changing simultaneously their internal configuration. They are formed now by interlinked domain walls of mixed orange (up-down-down) and red (up-up-up) triangles, as shown in Fig. 8. In this field region, colored triangles of the domain walls are in such proportion that the additional contribution to the total magnetization is averaged to zero, fluctuating around the value $M_s/3$ of the ordered green (gray) phase, as in the example of Fig. 8. Such fluctuations diminish by increasing N and the MCF.

Finally, for fields beyond the other boundary, $H=2.4$ T, the situation is quite different. Now the interlinked domain walls are formed mostly by red (dark) triangles (see Fig. 9) with a tendency to coalesce in small groups, or seeds, at the borders of the simulated clusters. This interesting feature of red (dark) seeds at the boundaries, as shown in Fig. 9, is a peculiar phenomenon quite similar to prenucleation phases,

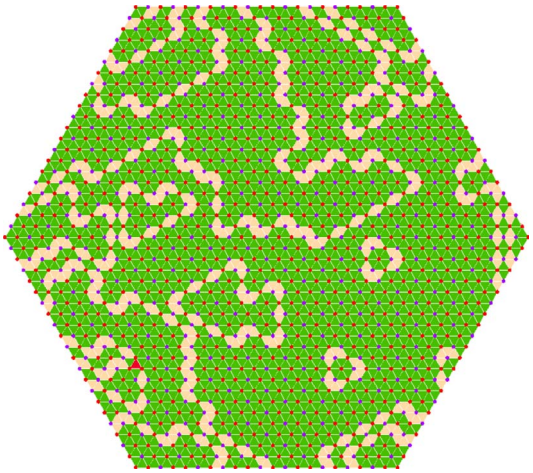

FIG. 7. (Color online) Snapshot of a particular configuration obtained in a hexagonal cluster of $N=1387$ spins, for the first plateau: $H=0.81$ T, at $T=4$ K and for 10^4 MCF (see red curve in Fig. 3). Notice the ordered green (gray) zone, with $M=M_s/3$, superimposed by interlinked domain walls, formed mostly by connected triangles in orange (light) color. These domain walls contribute to a reduction of the $M_s/3$ value of the green zone to a total $M=0.22M_s$ in this case.

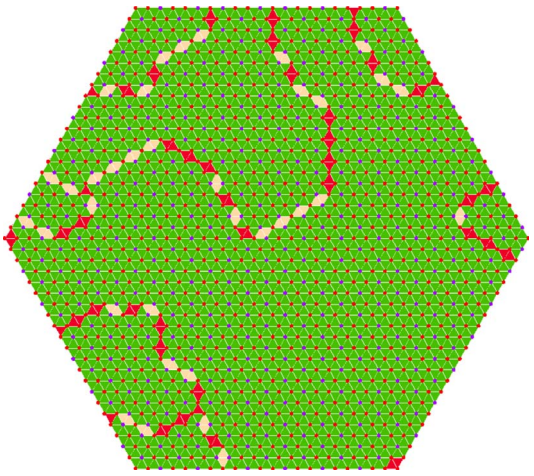

FIG. 8. (Color online) Snapshot of the second plateau at a field $H=2.0$ T. Other parameters as in Fig. 7. The total magnetization is $M=0.33M_s$ in this case. Observe now the extended green (gray) zone superimposed by interlinked domain walls of mixed orange (light) and red (dark) triangles. They are in a proportion that contribute almost zero extra moment. These domain walls are rather static across a finite window of the magnetic field: $1.2<H<2.4$ T.

as seen in heteronucleation,[37,38] in phase transformations,[39] and also in the kinetics of materials[40] of irreversible statistical mechanics studies. Proper nucleation in our simulation actually starts beyond the critical field ($H_c=3.6$ T) in the following way: first coalescence of small red (dark) seeds at the borders and then myriads of red (dark) seeds nucleating and growing, taking account of the whole cluster (in the bulk) until saturation. The nucleation process above H_c is a very rapid, disordered phenomenon that destroys the interlinked domain-wall structures seen in the former examples. Perfect alignment is only achieved at the end for fields higher than 4 T. This situation is better appreciated in the supplementary material (see Ref. 36).

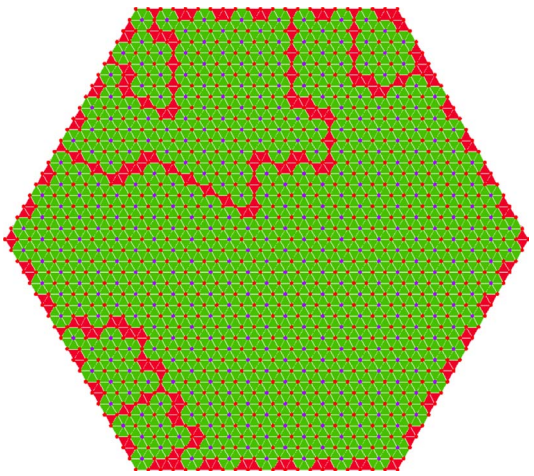

FIG. 9. (Color online) Snapshot of the third plateau, at a field $H=2.98$ T. Other parameters as in Figs. 7 and 8. The magnetic configuration is now formed by the green (gray) extended region of $M_s/3$, superimposed by domain walls in red (dark) color, giving a total magnetization of $M=0.41M_s$ in this case. Notice that some red (dark) seeds are distributed at the borders of the cluster, like in prenucleation phases of irreversible studies. Nucleation and growth of compact domains actually starts beyond the critical field, $H_c=3.6$ T.

All these nonequilibrium phenomena, just described above, were obtained for a particular sweep rate of 10^4 MCF. We tested various sweep rates, observing similar behavior for all of them, with a reduction in domain walls as the MCF increased. Beyond a sweep rate of 10^9 MCF none of these metastable interlinked domain walls were present. In that case, the disordered initial phase at zero field goes immediately to the 1/3 plateau, and above $H_c=3.6$ T to saturation. Such a 1/3 state was described solely by the green zone, without any domain wall, thus of long-range nature. The fact that our simulations ended up in the long-range ordered 1/3 plateau at equilibrium (at high MCF) at intermediate fields may be understood as a field-induced Kosterlitz-Thouless transition in the triangular Ising lattice, as explained theoretically in Ref.41. The required conditions, high fields and low temperatures, are fulfilled in the magnetization experiments in $Ca_3Co_2O_6$ and in our simulations. Such fixed critical region is thus guaranteed theoretically, see Ref. 42

Henceforth, we believe that our characterization of these metastable frustrated states, sweep-rate dependent, interlinked domain walls, must be related to the multiple-step phases of $Ca_3Co_2O_6$ found experimentally at low T, and which evolve over the (equilibrium) long-range ordered 1/3 plateau state, as seen in Figs. 7–9. An interesting task would be to find out the landscape of such local minima, where these metastable states survive (quasistatically) for rather long periods, allowing us to see them in the experiments and in the simulations.

V. TRIANGULAR QUANTUM CLUSTERS

In this section, we show how the 1/3 plateau of the Ising model of previous sections shares interesting similarities with the simplest quantum clusters of triangular geometry. A generic model for these 2D clusters is the following spin-$\frac{1}{2}$ Heisenberg Hamiltonian:

$$\mathcal{H}=\frac{1}{2}J\sum_{\langle i,j\rangle}^{N}\mathbf{S}_i\cdot\mathbf{S}_j-\delta\sum_{i}^{N}(\mathbf{S}_i\cdot\hat{\mathbf{n}})^2-g\mu_{\mathrm{B}}\sum_{i}^{N}\mathbf{S}_i\cdot\mathbf{H}, \quad (3)$$

where we have included an anisotropy term δ along the $\hat{\mathbf{n}}$ axis. Exact results, obtained with algebraic manipulators, for a triangular molecule ($N=3$) of parallel configuration $\hat{\mathbf{n}}\|\mathbf{H}$, are shown in Fig. 10. The thermal average of the total z component spin $M=\langle S^z\rangle$ is zero only at zero field, and it increases rapidly to the 1/3 plateau for any finite H, until some critical field $H_c\approx 0.03$ T, where it rapidly increases again to saturation. Such a transition is first order at $T=0$ only. Increasing the temperature produces a smooth growing up of M due to thermal fluctuations, as seen in Fig. 10. We should point out that very low temperatures and low fields are required to see the steps in the magnetization, since we have here a small quantum cluster ($N=3$) of spins $\frac{1}{2}$ with a very small interaction, $J=2.25$ μeV (as before). Results of the parallel configuration $\hat{\mathbf{n}}\|\mathbf{H}$ are independent of the anisotropy δ in this particular case.

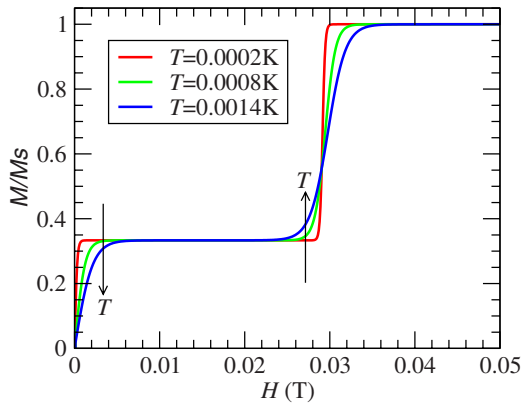

FIG. 10. (Color online) Exact magnetization versus magnetic field for the Heisenberg triangular molecule ($N=3$) and for different temperatures, as shown in the legend. We observe a tendency to form a 1/3 plateau. Other parameters used are $J=2.25$ μeV, $\delta=1$ μeV, and $S=\frac{1}{2}$. Notice the extremely low temperatures and low fields involved in this case.

Interesting to note in Fig. 10 is that such a trend resembles the Monte Carlo (MC) solution of the Ising model in the triangular lattice of the previous sections. Although it is not the same behavior, a tendency to form a 1/3 plateau is without any doubt. But, no further subplateaus can be observed in a triangular molecule because of lack of phase space. Domain walls in the Ising dynamics are minimally formed by triangles, as seen before.

Further supporting arguments come from numerical exact solutions on finite clusters. In Fig. 11, we see, for example, exact diagonalization results for the magnetization of the Heisenberg model in the triangular lattice, in the absence of anisotropy, at $T=0$, for $N=36$ and 39 sites.[43] The formation of a clear 1/3 plateau of finite width, $\Delta H=H_u-H_\ell$, is seen from the picture. Such results have been taken[44–47] as the numerical evidence of a definitive plateau in the thermodynamic limit: the bold blue (dark) line in Fig. 11 was drawn by connecting the midpoints of the finite-size steps for

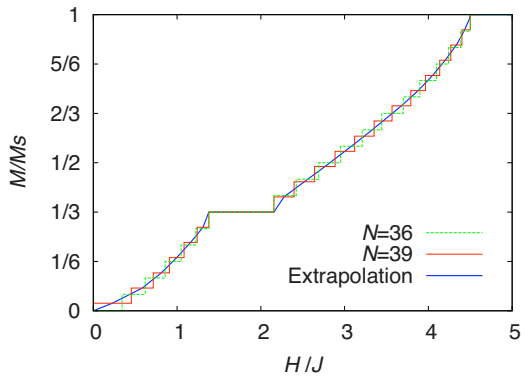

FIG. 11. (Color online) Exact diagonalization results for the magnetization versus magnetic field for isotropic Heisenberg quantum triangular clusters at $T=0$, $\delta=0$, and $S=\frac{1}{2}$. The dashed green (gray) and thin solid red (dark) lines are for $N=36$ and 39 sites, respectively, while the bold solid blue (dark) line is an extrapolation to the thermodynamic limit (see text). Notice the 1/3 plateau of finite width $\Delta H=0.78J$.

$N=39$ sites, except at the boundaries of the 1/3 plateau. A good estimate for the lower and upper fields of the boundaries of the exact 1/3 plateau in the triangular lattice were obtained by comparing spin wave and exact diagonalization results. They are given by $H_\ell=1.378J$ and $H_u=2.155J$, respectively. See Ref. 47 for further results.

To better see our point here, we should recall that both models, Ising and Heisenberg, show a similar behavior yet of different origin—with a 1/3 plateau—because the magnetic field in the Heisenberg case already breaks the symmetry from SU(2) to U(1), leaving the strong quantum fluctuations inoperable in the isotropic Heisenberg triangular case and, consequently, the $M=\frac{1}{3}$ state becomes a classical, collinear state, with long-range order, as in the Kosterlitz-Thouless transition mentioned above.

VI. CONCLUSION AND FINAL REMARKS

In summary, we did an extensive investigation of the triangular lattice using Monte Carlo simulations. We studied this lattice using a 2D Ising model of very large rigid magnetic moments coupled antiferromagnetically. We were motivated by multiple steps observed in the magnetization of the spin-chain $Ca_3Co_2O_6$ compound. We found very good agreement between our results and the experimental situation.[19] We demonstrated that the three observed plateaus of the ferrimagnetic phase (below $T\leq 10$ K) consist of metastable states and for this reason show time dependence. In the experimental results, such time dependence was observed on the sweep rate of the magnetic field, and in our case, this dependence comes from the number of MCF used on each step of the simulation. In fact, a close parallelism is found between these two approaches, as seen from the comparison of our Figs. 2–4 and Figs. 3, 4, and 5 from Ref. 19. Besides such agreement, we also found that in the limit of very large number of MCF, namely, at very slow sweep rate, the three plateaus converge into one, at $M/M_s=\frac{1}{3}$, like in the experiments, giving thus a thermal decay of these metastable states into the equilibrium 1/3 plateau, which has long-range order (the up-up-down green zone, with a hexagon as a unit cell).

Further analysis, using snapshots of some specific configurations, revealed the presence of interlinked (mobile) domain walls that give origin to the splitting of the 1/3 plateau below $T\leq 10$ K, as explained in the text. Such a result disproves the possibility of quantum tunneling as generating the multiple steps, at least for temperatures above 4 K, and for the reported sweep rates. Based on our results, we believe that at lower temperatures some arrested configurations may provide a slower dynamics of the domain walls, that could explain a T-independent time-decay process seen below 4 K, by critical slowing down, an aspect that must still be checked out.

Our solution was also investigated by considering the intrinsic dipolar interactions, finding no relevant contribution from such couplings. We therefore discarded them as possible generators of hysteresis phenomena, which are strongly present in the experiments[19] in the ferrimagnetic region. We believe that other ingredients or methods, like three-dimensional simulations, must be considered to deal with

such irreversible aspects, but this is beyond our model of the magnetization plateaus in $Ca_3Co_2O_6$.

Another important point that we wanted to emphasize in this work was linked to exact numerical solutions of the Heisenberg model in the triangular lattice on finite clusters. We did a comparison with our previous numerical classical Ising solution and found supporting arguments with the presence of the 1/3 plateau in the isotropic Heisenberg extreme quantum case of spin $\frac{1}{2}$ at $T=0$. Both models share the 1/3 plateau, although for different reasons. In the quantum-mechanical case the applied magnetic field strengthens the frustration effects of the triangular lattice up to a point of having sufficient overlap with the classical, collinear, threefold degenerate 1/3 plateau.[46] The crucial point here is that the presence of the 1/3 plateau in the isotropic quantum limit solution does not require a strong uniaxial anisotropy. Although we did not do a systematic thermal study of the exact solution of the Heisenberg model, we think that at low temperatures the 1/3 plateau would survive to thermal fluctuations in order to be observed numerically. Such a comparison, therefore, strongly supports our classical study of the spin-chain $Ca_3Co_2O_6$ compound.

Recently, it has come to our attention that similar results in the $Ca_3Co_2O_6$ system were obtained by Kudasov *et al.*[48] who also reproduced the ferrimagnetic steps in the magnetization using essentially the same 2D Ising model of frozen moments as described in this article, but with a different Glauber-type procedure. Although Kudasov *et al.* used periodic boundary conditions, while open boundary conditions and a single-flip Monte Carlo dynamics were employed in our calculations, our conclusions are similar. In addition to the results presented in Ref. 48, we explore the topology of the resulting triangular-based domain walls and attribute the value of the magnetization steps to their internal configuration. We also link the low-sweep rate results of the 1/3 plateau to a field-induced Kosterlitz-Thouless transition into the collinear, long-range-ordered equilibrium Ising state. Finally, we observe that the 1/3 plateau is also seen in the isotropic quantum case at $T=0$ on small clusters.

ACKNOWLEDGMENTS

This work was partially supported by FONDECYT (Chile) under Grant No. 1070224, CONICYT (Chile) Millennium Science Initiative under Project No. P06-022-F, and by CNPq (Brazil). One of us (G.M.) would like to acknowledge the Universidad Técnica Federico Santa María, in Valparaíso, Chile, for a pleasant sabbatical visit during 2008. We also thank Andreas Honecker for sharing his data on the triangular lattice.

*martinez@if.ufrgs.br
†vargas.patricio@gmail.com

[1] M. Oshikawa, M. Yamanaka, and I. Affleck, Phys. Rev. Lett. **78**, 1984 (1997).
[2] D. C. Cabra, A. Honecker, and P. Pujol, Phys. Rev. Lett. **79**, 5126 (1997).
[3] T. Vekua, D. C. Cabra, A. Dobry, C. Gazza, and D. Poilblanc, Phys. Rev. Lett. **96**, 117205 (2006).
[4] I. J. Hamad, L. O. Manuel, G. Martínez, and A. E. Trumper, Phys. Rev. B **74**, 094417 (2006).
[5] M. F. Collins and O. A. Petrenko, Can. J. Phys. **75**, 605 (1997).
[6] H. Fjellvåg, E. Gulbrandsen, S. Aasland, A. Olsen, and B. C. Hauback, J. Solid State Chem. **124**, 190 (1996).
[7] S. Aasland, H. Fjellvåg, and B. Hauback, Solid State Commun. **101**, 187 (1997).
[8] H. Kageyama, K. Yoshimura, K. Kosuge, H. Mitamura, and T. Goto, J. Phys. Soc. Jpn. **66**, 1607 (1997).
[9] A. Maignan, C. Michel, A. C. Masset, C. Martin, and B. Raveau, Eur. Phys. J. B **15**, 657 (2000).
[10] B. Martínez, V. Laukhin, M. Hernando, J. Fontcuberta, M. Parras, and J. M. González-Calbet, Phys. Rev. B **64**, 012417 (2001).
[11] B. Raquet, M. N. Baibich, J. M. Broto, H. Rakoto, S. Lambert, and A. Maignan, Phys. Rev. B **65**, 104442 (2002).
[12] V. Hardy, M. R. Lees, A. Maignan, S. Hébert, D. Flahaut, C. Martin, and D. M. Paul, J. Phys.: Condens. Matter **15**, 5737 (2003).
[13] R. Vidya, P. Ravindran, H. Fjellvåg, A. Kjekshus, and O. Eriksson, Phys. Rev. Lett. **91**, 186404 (2003).
[14] V. Hardy, S. Lambert, M. R. Lees, and D. McK. Paul, Phys. Rev. B **68**, 014424 (2003).
[15] M.-H. Whangbo, D. Dai, H.-J. Koo, and S. Jobic, Solid State Commun. **125**, 413 (2003).
[16] A. Maignan, V. Hardy, S. Hébert, M. Drillon, M. R. Lees, O. Petrenko, D. Mc K. Paul, and D. Khomskii, J. Mater. Chem. **14**, 1231 (2004).
[17] R. Frésard, C. Laschinger, T. Kopp, and V. Eyert, Phys. Rev. B **69**, 140405(R) (2004).
[18] V. Eyert, C. Laschinger, T. Kopp, and R. Frésard, Chem. Phys. Lett. **385**, 249 (2004).
[19] V. Hardy, M. R. Lees, O. A. Petrenko, D. McK. Paul, D. Flahaut, S. Hébert, and A. Maignan, Phys. Rev. B **70**, 064424 (2004).
[20] D. Flahaut, A. Maignan, S. Hébert, C. Martin, R. Retoux, and V. Hardy, Phys. Rev. B **70**, 094418 (2004).
[21] V. Hardy, D. Flahaut, M. R. Lees, and O. A. Petrenko, Phys. Rev. B **70**, 214439 (2004).
[22] A. Villesuzanne and M.-H. Whangbo, Inorg. Chem. **44**, 6339 (2005).
[23] K. Takubo, T. Mizokawa, S. Hirata, J.-Y. Son, A. Fujimori, D. Topwal, D. D. Sarma, S. Rayaprol, and E.-V. Sampathkumaran, Phys. Rev. B **71**, 073406 (2005).
[24] K. Yamada, Z. Honda, J. Luo, and H. Katori, J. Alloys Compd. **423**, 188 (2006).
[25] Hua Wu, M. W. Haverkort, Z. Hu, D. I. Khomskii, and L. H. Tjeng, Phys. Rev. Lett. **95**, 186401 (2005).
[26] Hua Wu, Z. Hu, D. I. Khomskii, and L. H. Tjeng, Phys. Rev. B **75**, 245118 (2007).
[27] W. Wernsdorfer, M. Murugesu, and G. Christou, Phys. Rev. Lett. **96**, 057208 (2006).
[28] M. R. Wegewijs, C. Romeike, H. Schoeller, and W. Hofstetter,

New J. Phys. **9**, 344 (2007).
[29] For a review, see *Quantum Tunneling of Magnetization*, edited by L. Gunther and B. Barbara (Kluwer, Dordrecht, 1995).
[30] Yuri B. Kudasov, Phys. Rev. Lett. **96**, 027212 (2006).
[31] X. Y. Yao, S. Dong, and J.-M. Liu, Phys. Rev. B **73**, 212415 (2006).
[32] X. Y. Yao, S. Dong, H. Yu, and J.-M. Liu, Phys. Rev. B **74**, 134421 (2006).
[33] M. Vázquez, K. Nielsch, P. Vargas, J. Velázquez, D. Navas, K. Pirota, M. Hernández-Velez, E. Vogel, J. Cartes, R. B. Wehrspohn, and U. Gosele, Physica B **343**, 395 (2004).
[34] M. Vázquez, M. Hernández-Velez, K. Pirota, A. Asenjo, D. Navas, J. Velázquez, P. Vargas, and C. Ramos, Eur. Phys. J. B **40**, 489 (2004).
[35] D. P. Landau and K. Binder, *A Guide to Monte Carlo Simulations in Statistical Physics*, 2nd ed. (Cambridge University Press, Cambridge, England, 2005).
[36] See EPAPS Document No. E-PRBMDO-79-041918 for the time evolution of domain walls within a single sweep rate of the magnetic field until saturation. For more information on EPAPS, see http://www.aip.org/pubservs/epaps.html.
[37] H. Vehkamäki, *Classical Nucleation Theory in Multicomponent Systems* (Springer, Berlin, 2006).
[38] C. Sagui and M. Grant, Phys. Rev. E **59**, 4175 (1999).
[39] D. A. Porter and K. E. Easterling, *Phase Transformations in Metals and Alloys* (Chapman and Hall, London, 1992).
[40] R. W. Balluffi, S. M. Allen, W. Craig Carter, and R. A. Kemper, *Kinetics of Materials* (John Wiley and Sons, New York, 2005).
[41] H. W. J. Blöte, M. P. Nightingale, X. N. Wu, and A. Hoogland, Phys. Rev. B **43**, 8751 (1991).
[42] H. W. J. Blöte and M. P. Nightingale, Phys. Rev. B **47**, 15046 (1993).
[43] A. Honecker (private communication).
[44] B. Bernu, P. Lecheminant, C. Lhuillier, and L. Pierre, Phys. Rev. B **50**, 10048 (1994).
[45] A. Honecker, J. Phys.: Condens. Matter **11**, 4697 (1999).
[46] A. Honecker, J. Schulenburg, and J. Richter, J. Phys.: Condens. Matter **16**, S749 (2004).
[47] *Quantum Magnetism*, edited by U. Schollwöck, J. Richter, D. J. J. Farnell, and R. F. Bishop (Springer, Berlin, 2004).
[48] Yu. B. Kudasov, A. S. Korshunov, V. N. Pavlov, and D. A. Maslov, Phys. Rev. B **78**, 132407 (2008).